

Plasma separation and preparation on centrifugal microfluidic disk for blood assays

Ju-Nan Kuo · Xuan-Fu Chen

Received: 6 October 2014 / Accepted: 6 January 2015 / Published online: 10 January 2015
© Springer-Verlag Berlin Heidelberg 2015

Abstract The present study proposes a simple lab-on-CD device in which the plasma is first separated from the whole human blood, then divided into two samples of equal volume, and finally decanted into a detection chamber for analysis purposes. The performance of the proposed device is then evaluated using blood samples with hematocrit concentrations ranging from 6 to 48 %. The results show that for a blood sample with a hematocrit concentration of 6 %, a separation efficiency of 96 % can be achieved within 5–6 s. Moreover, the two plasma samples collected from the left and right branches of the optimized Y-shaped splitter network differ in volume by no more than 0.5 nL. It is shown that the volume of plasma decanted into the detection chamber can be precisely controlled through an appropriate manipulation of the disk rotation speed. Finally, the practical feasibility of the proposed device is demonstrated by performing a creatinine test, the linear dynamic range show that it can be used for creatinine detection in blood assay. In this study, systematical evaluation on the functionality and performance of such a device has been done. The merits of this device are its low cost, straightforward fabrication process, low sample consumption, and high portability.

1 Introduction

Blood tests are one of the most common clinical diagnostic procedures. The first step in performing a blood test is

generally to separate the blood plasma (or cell-free serum) from the whole human blood so as to remove the blood cells and cellular components (Toner and Irimia 2005), which may otherwise confuse the analysis results (Yager et al. 2006). The separation process is generally performed in a laboratory using bench-top centrifugation equipment. However such an approach is expensive, labor intensive and time-consuming. Furthermore, having separated the blood plasma, it must then be extracted from the combined plasma/blood cell reservoir and transferred to another device for further preparation and analysis. In practice, the plasma separation and analysis procedures can take up to several hours to complete, and require the intervention of qualified technical personnel. However, with growing interest in the development of point-of-care (POC) applications, there is an urgent need for rapid, straightforward and low-cost automated systems capable of performing the complete plasma separation and preparation process in a more seamless and efficient manner.

Microfluidic systems involves deal with fluid flow (Hajmohammadi and Nourazar 2014; Hajmohammadi et al. 2014a) and optimization (Hajmohammadi et al. 2013a, b, 2014b) have attracted considerable attention due to their potential for the development of highly integrated systems capable of performing parallel sample handling and analysis on a single microchip. Such lab-on-a-chip (LoC) devices have many advantages over their large-scale counterparts, including a lower sample/reagent consumption, a faster response time, a greater portability, a lower cost, and so on. LoC devices provide the means to perform multiple sample preparation steps (e.g., separation, decanting, metering, and mixing) on a single platform (Vilkner et al. 2004). Consequently, they are ideally suited to POC applications, in which the entire assay protocol needs to be carried out in a seamless and low-cost way (Tüdös et al. 2001;

J.-N. Kuo (✉) · X.-F. Chen
Department of Automation Engineering,
National Formosa University, No. 64, Wenhua Rd.,
Huwei, Yunlin 632, Taiwan
e-mail: junan@nfu.edu.tw

X.-F. Chen
e-mail: a66237@yahoo.com.tw

Arora et al. 2010). The literature contains many methods for performing blood separation (Kersaudy-Kerhoasa and Sollierb 2013) in microfluidic chip. Zhang et al. (2012) proposed a continuous on-chip plasma separation method based on the natural aggregating and sedimentation behavior of red blood cells at low shear rate. Sedimentation is sometimes used in specific-to-purpose microchannel structures (Huang et al. 2010) or combination with trenches to speed up the plasma extraction process (Dimov et al. 2011). Microfiltration is simply based on particle size differences and selective segregation by well-dimensioned pores for blood separation method that using built-in porous filters (Moorthy and Beebe 2003), cross-flow filters (Van Delinder and Groisman 2006; Chen et al. 2007), and Magnetically-actuated blood filter unit (Chung et al. 2012). In addition, various solutions are available for plasma extraction at the microfluidic device depending on the dielectrophoresis force (Huang et al. 2002), magnetic-activated cell separation (Inglis et al. 2004; Smistrup et al. 2005), acoustic force (Petersson et al. 2005), non-inertial force (Tsutsui and Ho 2009), hydrodynamic field effect (Lee et al. 2013; Sun et al. 2013), capillary-driven contactless dielectrophoresis (Chen et al. 2014), and so on. However, such methods were designed for continuous blood separation, or involve a complex fabrication process for the device.

Centrifugal microfluidic devices, commonly referred to as Lab-on-a-CD (Madou et al. 2006; Gorkin et al. 2010), employ the centrifugal force generated as the CD rotates to drive the sample through the microchannel. Such devices do not require external pumps to accomplish fluid transport, and therefore greatly reduce the number of physical connections required to realize the device. As a result, centrifugal microfluidic devices have attracted significant attention in the literature as a means of performing such mainstream diagnostic applications (Cho et al. 2007; Li et al. 2009), as molecule assays (Steigert et al. 2006, 2007), nucleic acid analyses (Focke et al. 2010; Lutz et al. 2010), and enzyme linked immunosorbent assays (Lai et al. 2004; He et al. 2009; Lee et al. 2009). Importantly, centrifugal microfluidic devices provide a feasible means of performing multiple fluidic functions, including valving (Badr et al. 2002), metering (Andersson et al. 2007), and mixing (Grumann et al. 2005; Ducrée et al. 2005; La et al. 2013). Consequently, they provide a promising solution for the development of low-cost LoC systems capable of performing the entire sample preparation and analysis procedure on a single chip.

Existing Lab-on-a-CD devices for performing human blood assays exploit the difference in the mass density of the different components of human blood to separate the plasma from the blood cells, the basic laws governing a centrifugal separation process are presented (Haeberle et al. 2006; Zhang et al. 2008), and then use a plasma-skimming

technique (Kuo and Li 2014) to extract a small amount of plasma for analysis purposes. In such an approach, the blood cells and plasma are separated into different phase layers under the effects of centrifugation and sedimentation, but remain within the same reservoir. By contrast, in the centrifugal Lab-on-a-CD device proposed in the present study, the blood cells and plasma flow into two different reservoirs as the CD rotates. As a result, the need for a skimming process to retrieve the plasma sample is removed. Having separated the plasma, the CD rotation speed is increased, thereby causing the plasma to flow through a Y-shaped microchannel designed in such a way as to divide the sample into two smaller samples of equal volume. Finally, through a further manipulation of the CD rotation speed, a portion of the plasma sample is decanted into a detection chamber for further preparation and analysis purposes. Overall, the proposed device provides a convenient and rapid means of performing complete blood assays on a single platform, irrespective of the size of the blood sample collected.

2 Experimental design and method

2.1 Plasma separation microchannel

Figure 1 presents a schematic illustration of the microchannel network patterned on the microfluidic disk. As shown, the microchannel network comprises a plasma separation network and a splitter/decantation network. The plasma

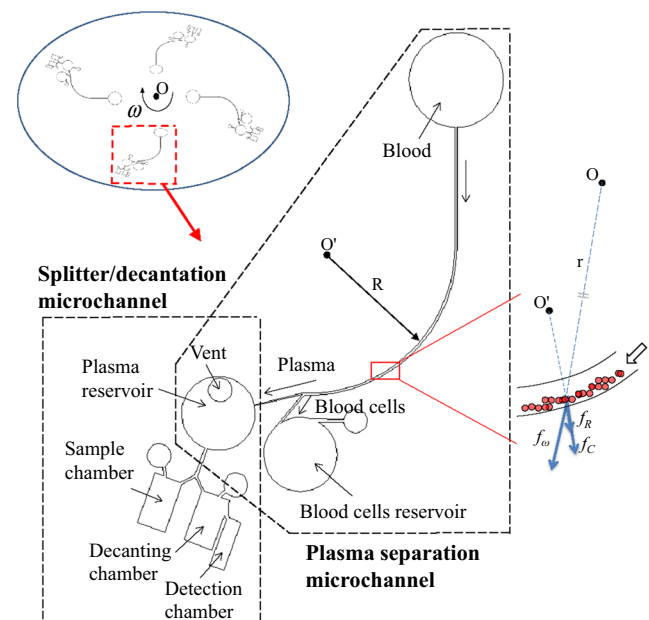


Fig. 1 Schematic illustration of microchannel network configuration on proposed Lab-on-a-CD device

separation network consists of a straight microchannel, a curved microchannel and a branched microchannel (Kuo and Li 2014). As the disk rotates, the blood within the separation network is subjected to three different body forces, namely the centrifugal force f_ω due to system rotation, the Coriolis force f_C due to the combined effects of the system rotation and the liquid velocity, and the centrifugal force f_R generated by the microchannel curvature itself. In the straight region of the separation network, the Coriolis force is the only force acting on the sample. As a result, only a minor separation of the plasma and blood cells occurs. However, in the curved region of the network, the sample is subjected to all three body forces, and the blood cells are driven toward the outer wall of the microchannel as a result of their greater density. Thus, on reaching the bifurcation point at the end of the curved channel, the blood cells flow into the blood cell reservoir, while the plasma continues in the downstream direction. Note that in designing the separation microchannel network, the width of the channel leading from the bifurcation point to the blood cell reservoir is deliberately assigned a greater value than that of the plasma channel leading in the downstream direction. Thus, the separation process at the bifurcation point is enhanced by the so-called Zweifach-Fung effect (Fung 1973), which causes the cells to be drawn into the blood cell microchannel as a result of the greater flow rate.

The centrifugal force f_ω , Coriolis force f_C , and second centrifugal force f_R developed in the plasma separation microchannel network as the CD rotates are given by (Zhang et al. 2008)

$$f_\omega = r\rho\omega^2, \tag{1}$$

$$f_C = 2\rho\omega u, \tag{2}$$

$$f_R = \rho u^2/R, \tag{3}$$

where r is the distance from the rotation center to the point of interest, ρ is the density of the blood component, ω is the angular rotation speed, u is the liquid velocity, and R is the radius of curvature of the curved microchannel. Plasma separation mainly occurs in the curved microchannel, where the centrifugal force f_ω , the Coriolis force f_C and the second centrifugal force f_R all contribute to plasma separation. In addition, the Zweifach-Fung effect plays a minor role since it only affects blood cells at the bifurcation point of the curved microchannel.

2.2 Splitter/decantation microchannel

Having separated the plasma from the blood cells, the CD rotation speed is increased in order to divide the plasma into two samples of equal volume by means of a Y-shaped splitter channel. Note that the separation of the sample into two

smaller equal-volume samples is of great practical importance since it enables a quantitative plasma assay to be performed (Gao et al. 2011). As shown in Fig. 2, the plasma splitter/decantation network on the proposed Lab-on-a-CD device comprises the plasma reservoir, the Y-shaped splitter channel, a sample chamber, a decanting chamber, and a detection chamber. In the straight microchannel connecting the plasma reservoir and the Y-shaped splitter channel, the Coriolis force f_C is the only active force. However, in the two branches of the splitter network, all three body forces (i.e., f_ω , f_C , and f_R) act simultaneously. The Coriolis force generated as the disk rotates causes a nonequal division of the plasma flow between the two branches of the splitter network when the microchannels are assigned the same geometry parameters (Kuo et al. 2012). For example, the flow rate in the left branch is lower than that in the right branch when the disk rotates in the clockwise direction. Accordingly, a series of computational fluid dynamics (CFD) simulations were performed to determine the optimal geometry parameters of the left and right branches in the Y-shaped network. Note that in optimizing the design of the splitter network, the simulations considered both the inclination angle and the width of the two branches of the Y-shaped channel.

Decanting plasma from the centrifuged blood is an important preparation procedure when performing blood biochemical assays. As described above, in the Lab-on-a-CD device proposed in the present study, the plasma is deposited in the decanting chamber by means of an

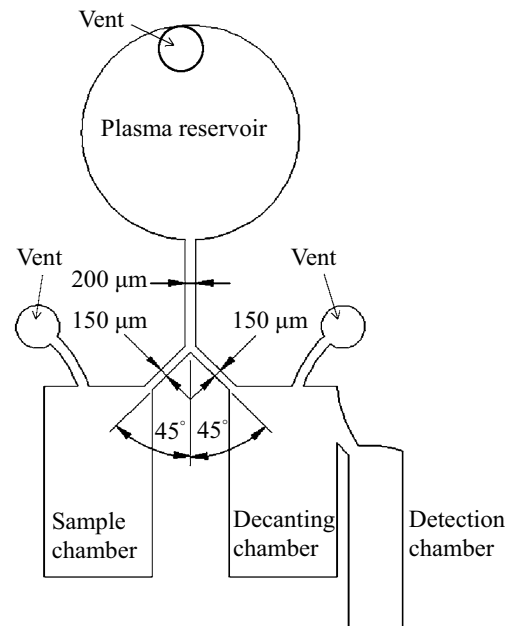


Fig. 2 Schematic illustration of Y-shaped splitter/decantation microchannel network

equal plasma flow division process. Having deposited the plasma, the rotational speed of the CD is further increased; thereby generating an inertial force which causes some of the plasma in the decanting chamber to overflow into the detection chamber. Notably, the volume of plasma decanted into the detection chamber can be precisely controlled by adjusting the rotational speed of the CD.

2.3 Fabrication process

The microfluidic disk was fabricated using conventional soft lithography techniques. Briefly, photomask patterns for the plasma separation network and splitter/decantation network were generated using AutoCAD software and transferred to a clear transparent film. A photolithography technique was then used to fabricate an SU-8 master of the total microchannel network. The master was used to transfer the microchannel network to a poly(dimethylsiloxane) (PDMS) layer with a thickness of 50 μm . A via hole with a diameter of 2 mm was drilled in the inlet reservoir region of the PDMS layer to serve as an inlet for the blood sample. In addition, several vents (each with a diameter of 1 mm) were drilled in the blood cell, plasma, sample and decanting reservoirs/chambers of the microchannel network in order to balance the pressure during CD rotation. The PDMS layer was carefully positioned on a CD (diameter 12.7 cm) and was then bonded to the surface by means of an oxygen plasma process involving an initial curing procedure (70 $^{\circ}\text{C}$ for 3 h), an oxygen plasma treatment process, and a plasma cleaning operation (Harrick, PDC-001).

Referring to Fig. 1, the blood reservoir had a diameter of 6.4 mm, while the blood cell and plasma reservoirs each had a diameter of 5 mm. The straight channel in the separation network had a length of 8 mm, while the curved channel had a radius of 10 mm. Both channels had a width of 160 μm . To induce the Zweifach-Fung effect at the bifurcation point of the branched microchannel, the width of the channel leading to the blood cell reservoir was set as 100 μm , while that of the channel leading to the plasma reservoir was set as 60 μm . In the splitter/decantation microchannel network, the sample and decanting chambers each had dimensions of 3.5 mm \times 2 mm, while the detection chamber measured 3.4 mm \times 1 mm. Finally, the default dimensions of the Y-shaped splitter channel were set as shown in Fig. 2. Note that all of the microchannels, reservoirs and chambers on the microfluidic disk had a depth of 50 μm .

2.4 Experimental setup

The whole human blood used in the present experiments was drawn from a healthy male donor and pretreated with the anticoagulant EDTA. The blood was then diluted

with PBS (phosphate buffer saline) to designated hematocrit concentration levels in the range of 6–48 %. A blood sample with a volume of 1.0 μL was introduced into the blood inlet reservoir using a pipette. The disk was then placed on a spin processor (SP-M2-P, APISC) and rotated in the clockwise direction. Based on experimental observations, the plasma separation and equal-volume division processes were performed at disk rotation speeds of 1,800 and 2,000 rpm, respectively, while the decanting process was performed using a disk rotation speed in the range of 2,200–3,000 rpm. The efficiency of the plasma separation process was evaluated as follows: (Zhang et al. 2008)

$$\eta = (C_{FC} - C_{PC})/C_{FC}, \quad (4)$$

where C_{FC} is the cell concentration in the blood inlet reservoir and C_{PC} is the cell concentration in the plasma reservoir. Cell concentration was determined by cell counting.

The flow behavior of the plasma during the separation, division and decanting processes was observed using an image acquisition system comprising a stroboscope (DT-311 N, SHIMPO), a triggering sensor, and a high-speed charge-coupled device (CCD) camera (EO-0413C, Edmund Optics). (Note that the sensor synchronized the stroboscope with the disk rotation speed by detecting the signals reflected from a trigger mark on the surface of the disk.) The captured images were analyzed using digital image processing software in order to evaluate the experimental results.

3 CFD simulations

As described in Sect. 2.2, the plasma flow rates within the two branches of the Y-shaped splitter channel are non-equal when the branches are assigned identical geometry parameters due to the Coriolis force effect. Therefore, the geometry of the Y-shaped splitter must be carefully designed so as to achieve an equal division of the plasma sample; thereby enabling a quantitative assay to be performed. Accordingly, in the present study, the optimal geometry parameters of the splitter microchannel were determined via a series of CFD simulations performed using commercial COMSOL finite element analysis software. “The plasma reservoir, the Y-shaped splitter channel with a sample chamber and a decanting chamber were chosen as the computational domain. The different number of grids ranged from 12,000 to 90,000 were tested to verify the solution is grid-independent. The results have shown that the structured grids with 81,646 elements yield the optimal number of grids.”

In performing the plasma division and decanting simulations, the fluid within the microchannel network was assumed to consist of plasma and air. The density and viscosity of the air were specified as 1.164 kg/m^3 and 1.84×10^{-5} Ns/m^2 , respectively; while the density and

viscosity of the plasma were specified as $1,025 \text{ kg/m}^3$ and $1.5 \times 10^{-3} \text{ Ns/m}^2$, respectively. Moreover, the hydrostatic pressure developed within the plasma reservoir as a result of rotation was taken into account. Fixed-pressure boundary conditions were imposed at the inlet and outlet channels and a no-slip boundary condition was applied on all the channel walls. The body force acting on the fluid in the splitter/decantation microchannel network comprises three different components, namely, the gravity force, centrifugal force, and Coriolis force. Thus, in the present simulations the governing equations were specified as follows:

$$\nabla \cdot \mathbf{V} = 0, \tag{5}$$

$$\rho \left[\frac{\partial \mathbf{V}}{\partial t} + (\mathbf{V} \cdot \nabla) \mathbf{V} \right] = \mathbf{F} - \nabla p + \mu \nabla^2 \mathbf{V}, \tag{6}$$

$$\mathbf{F} = \rho \mathbf{g} + \mathbf{F}_{ce} + \mathbf{F}_{co} = \rho \left(\mathbf{g} + \mathbf{r}|\omega|^2 - 2\omega \cdot \mathbf{V} \right), \tag{7}$$

where \mathbf{V} is the velocity vector, \mathbf{g} is the gravity vector, \mathbf{r} is the radial position vector, and ω is the angular velocity vector.

4 Results and discussion

4.1 Separation results

The plasma separation performance of the microfluidic disk was evaluated using a $1.0 \mu\text{L}$ diluted whole blood sample with a hematocrit concentration of 6 %. The burst frequency of the blood inlet valve was observed to be around 1,650 rpm. Thus, in performing the separation process, the disk rotation speed was specified as 1,800 rpm. It was found that the plasma within the whole blood sample was separated from the cells within 5–6 s. The separation performance was also evaluated at higher rotation speeds of up to 2,000 rpm. However, no noticeable increase in the separation efficiency was observed. Thus, the CD rotation speed was set as 1,800 rpm in all of the subsequent plasma separation tests.

Figure 3 presents experimental images of the plasma separation process. Due to their higher density, the blood cells within the sample move toward the outer wall of the curved microchannel under the effects of the three body forces (see Fig. 3a) and subsequently enter the blood cell reservoir when reaching the bifurcation point (see Fig. 3b). By contrast, the plasma continues to flow in the downward direction, and subsequently enters the plasma reservoir (see Fig. 3c). A close examination of Fig. 3a and c shows that very few blood cells remain within the plasma as it flows past the bifurcation point and enters the plasma reservoir. Notably, the plasma separation effect is largely completed within the curved microchannel. Thus, the Zweifach-Fung

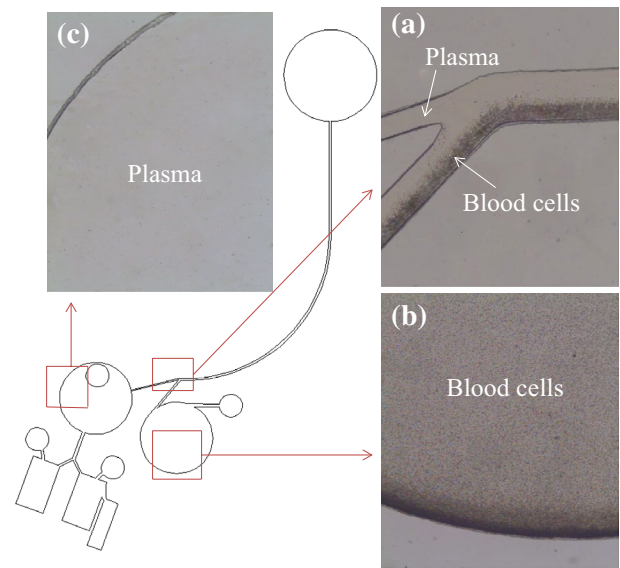


Fig. 3 Experimental observations of blood plasma separation process: **a** separation of blood cells and plasma at bifurcation point, **b** collection of blood cells in blood cell reservoir, and **c** collection of nearly pure plasma in plasma reservoir

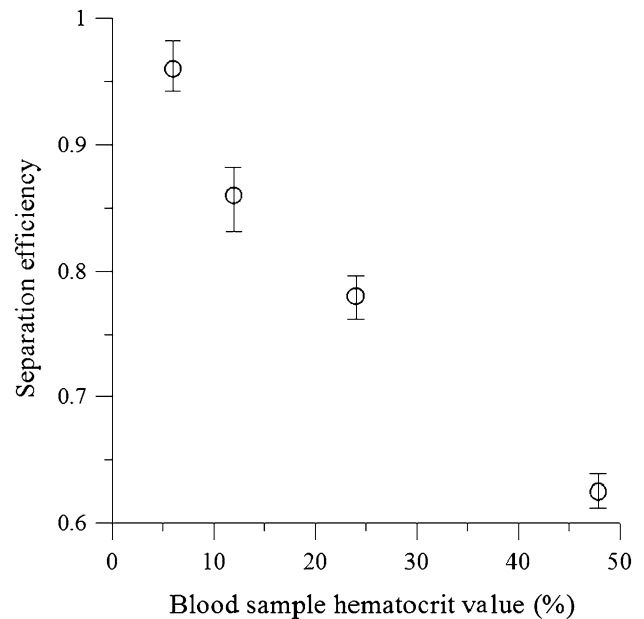


Fig. 4 Plasma separation efficiency for blood samples with different hematocrit concentrations

effect exerts only a very minor effect on the plasma as it passes the bifurcation point. Overall, the experimental images shown in Fig. 3 confirm the effectiveness of the proposed curved microchannel design in achieving a thorough separation of the blood plasma from the blood cells.

Figure 4 shows the separation efficiency of the proposed microfluidic disk for various hematocrit concentrations in

the range of 6–48 %. The separation efficiency for a blood sample with a hematocrit concentration of 6 % is seen to be 96 %. It is noted that this value is higher than that reported by Blatter et al. (2005) for a blood sample with a hematocrit concentration of 5 % (i.e., 90 %). It is thought that the superior separation performance of the proposed device is due to the combined effects of the three different body forces. In addition, it is noted that while the separation efficiency is less than that of the centrifugal extraction scheme proposed by Haeberle et al. (2006), i.e., 99 %, the plasma sample obtained using the proposed device is nevertheless suitable for most clinical blood tests. For example, many tests involve simply diluting blood plasma to a certain ratio and then performing a colorimetric reaction. Furthermore, in some tests (e.g., those for rheumatoid factors), a 100 % pure plasma sample is not required since the concentration of the target substance is relatively high.

It is seen in Fig. 4 that the separation efficiency reduces monotonically with an increasing hematocrit concentration. For example, given a hematocrit concentration of 12 %, the separation efficiency reduces to 87 %, while for a hematocrit concentration of 48 % (whole blood), the separation efficiency is just 62 %. The reduction in the separation performance with an increasing hematocrit concentration is to be expected since the intensity of the interactions among the blood cells increases as the number of cells increases. Moreover, blood with a higher hematocrit concentration has a higher viscosity, and thus flows more slowly. Consequently, both the Coriolis force f_C and the second centrifugal force f_R are also reduced. It is noted that the separation efficiency of the proposed disk may also be affected by such issues as the ambient temperature, the smoothness and hydrophilicity of the microchannel surface, and so on. For example, it was reported by Zhang et al. (2008) that the separation efficiency in PDMS microchannels increases with an increasing temperature due a reduction in the sample viscosity.

4.2 Splitter/decantation results

A plasma sample with a volume of around 0.4–0.5 μL was deposited in the plasma reservoir by performing a blood separation test using a CD rotation speed of 1,800 rpm. The plasma was then divided using the Y-shaped splitter network shown in Fig. 2 by increasing the CD rotation speed to 2,000 rpm. Figure 5a and b show the numerical and experimental results obtained for the plasma division process. From inspection, the volume of the plasma sample obtained from the left branch of the splitter network is approximately 17.5 nL lower than that obtained from the right branch of the network. In other words, the results confirm that for a clockwise rotation of the CD, the Coriolis force reduces the flow rate in the left branch of the splitter

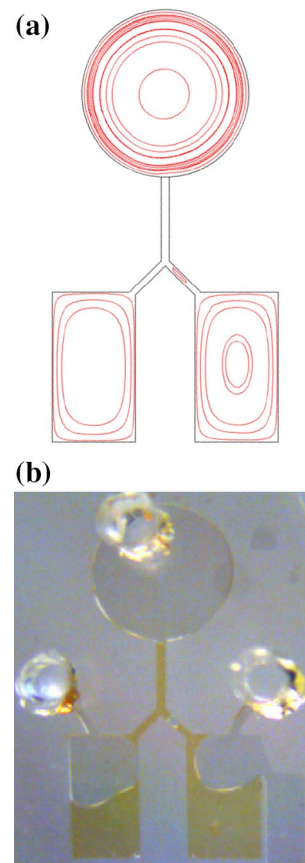


Fig. 5 **a** CFD simulation results for flow fields in Y-shaped splitter network, and **b** experimental results showing nonequal division of plasma between two branches

network when the two channels have an identical geometry (i.e., the same inclination angle and width).

In optimizing the geometry parameters of the Y-shaped splitter network, the parameters of the straight channel and left branches were assigned the values shown in Fig. 2, and the equality of the sample division was then calculated for the inclination angle and channel width of the left branch were assigned values in the ranges of 35°–45° and 150–170 μm , respectively, and the difference in the collected plasma volumes in the two reservoirs was evaluated by means of CFD simulations. Note that in determining the optimal inclination angle, the channel width was assigned a constant value of 150 μm (see Fig. 2), while in optimizing the channel width, the inclination angle was assigned a constant value of 45°. Furthermore, all of the remaining geometry parameters in the microchannel network were assigned the values shown in Fig. 2. The corresponding results obtained for the difference in volume of the two samples collected from the left and right branches, respectively, are presented in Fig. 6a and b. It is seen that the optimal value of the left branch inclination angle is equal to 41°, while the optimal value of the left branch channel

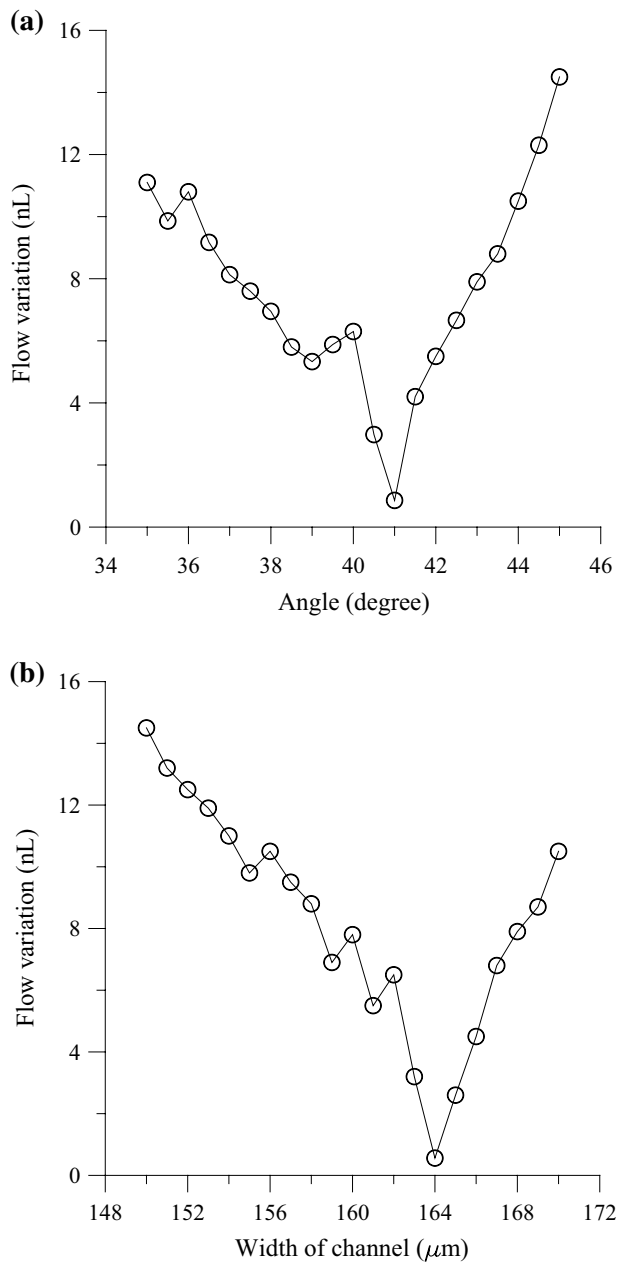


Fig. 6 Flow volume difference as function of left branch geometry parameters: **a** inclination angle, and **b** channel width

width is $164\ \mu\text{m}$. Given an inclination angle of 41° , the difference in the volume of plasma collected from the left and right branches is less than $0.53\ \text{nL}$, while for a channel width of $164\ \mu\text{m}$, the difference in the collected plasma volumes is $0.35\ \text{nL}$.

Figure 7 shows the experimental results for the plasma division within the optimized Y-shaped splitter networks. From inspection, the difference between the plasma volumes in the left and right reservoirs is found to be around $0.50\ \text{nL}$ for an inclination angle of 41° and $0.25\ \text{nL}$ for a

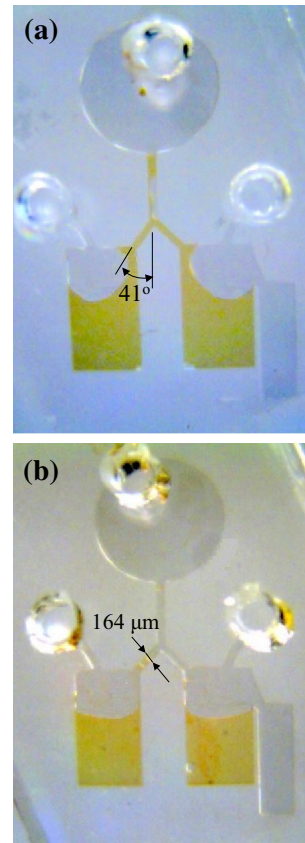


Fig. 7 Experimental results showing equal division of plasma between two branches in optimized Y-shaped splitter networks: **a** inclination angle of 41° , and **b** channel width of $164\ \mu\text{m}$

channel width of $164\ \mu\text{m}$, respectively. As a result, the effectiveness of the optimized network designs in achieving an equal division of the plasma is confirmed.

As described above, in the proposed microfluidic disk, the plasma is divided into two equal-volume samples by setting the CD rotational speed to $2,000\ \text{rpm}$. A small volume of plasma in the decanting reservoir is then flowed into the detection chamber by increasing the rotational speed to a value in the range of $2,200\text{--}3,000\ \text{rpm}$. Importantly, the flow resistance imposed by the splitter microchannel throtles the sample chamber, and thus only the plasma in the decanting chamber overflows into the detection chamber as the disk rotates. The experimental images presented in Fig. 8 confirm that the decanted volume increases with an increasing rotation speed. Figure 9 shows the numerical and experimental results for the decanted volume as a function of the disk rotation speed. The two sets of results deviate by no more than 3% . Thus, the effectiveness of the experimental splitter/decantation network is confirmed. It is observed that a near perfect linear relationship exists between the decanted volume and the CD rotation speed. From inspection, the gradient (i.e., the decanting rate) is

Fig. 8 Experimental images showing decanted volumes at different disk rotation speeds

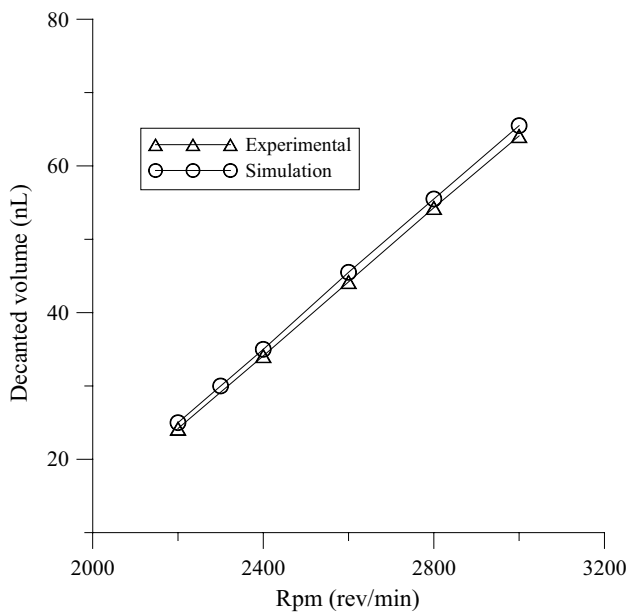
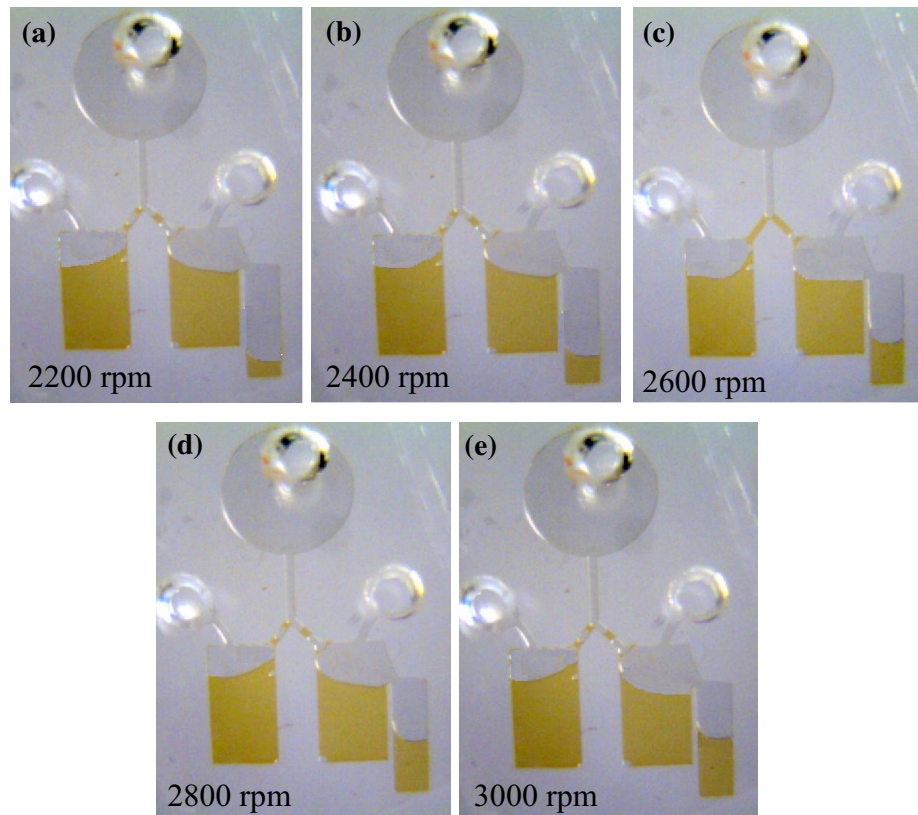


Fig. 9 Variation of decanted volume with disk rotation speed

found to be around 0.05 nL/rpm. In other words, the results confirm that the CD rotation speed provides an effective means of metering highly precise volumes of sample into the detection chamber for further on-disk processing and/or testing.

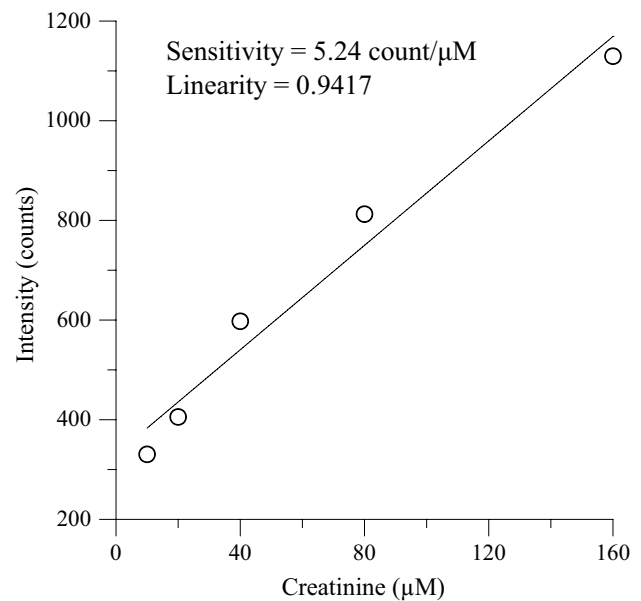


Fig. 10 Variation of intensity with different creatinine concentrations

4.3 Creatinine test

Creatinine is the final byproduct of muscle metabolism in mammalian cells that is excreted unchanged by the kidneys. Therefore, it is an important indicator of renal health

in blood tests. The normal range for serum/plasma creatinine is 45–110 μM and its concentration is not very much affected by diet changes. The ability of the lab-on-CD device fabricated in the present study to produce plasma samples into the detection chamber suitable for quantitative blood assays was evaluated by measuring the creatinine intensity of the plasma separated from whole blood samples containing different concentrations of creatinine assay kit (KA0849, Abnova). In the assay, creatinine is converted to generate red color (wavelength of 570 nm) and the signals are collected by a spectrometer (USB2000+, Ocean Optics). Figure 10 shows the variation of the intensity of the separated plasma with the concentration of creatinine added to the whole blood sample. It is seen that the intensity increases with an increasing creatinine concentration at concentrations of less than approximately 160 μM . In the concentration range shows that a slope of calibration curve is 5.24 count/ μM , and a near linear relationship (linearity = 0.9417) exists between the intensity and the creatinine concentration can be reliably detected.

5 Conclusions

This study has proposed a centrifugal microfluidic disk for the separation and preparation of blood plasma samples. In the proposed device, the plasma is separated from the whole human blood using a disk rotation speed of 1,800 rpm and is flowed into a plasma collection chamber. The disk rotation speed is then increased to 2,000 rpm in order to divide the collected plasma into two smaller equal-volume samples by means of a Y-shaped splitter channel. Finally, the disk rotation speed is further increased to a value in the range of 2,200–3,000 rpm in order to decant a small volume of the plasma into a detection chamber for further preparation and analysis purposes. The performance of the proposed device has been evaluated both numerically and experimentally. The experimental results have shown that a plasma separation efficiency of up to 96 % can be achieved within 5–6 s given a diluted blood sample with a hematocrit concentration of 6 %. Moreover, it has been shown that the separation efficiency increases monotonically as the hematocrit concentration decreases. The simulation and experimental results have shown that the volumes of the two plasma samples collected from the two branches of the Y-shaped splitter channel differ by no more than 0.5 nL given an optimal (i.e., non-symmetrical) design of the left and right branches. Moreover, by carefully manipulating the disk rotation speed, a precise volume of plasma can be decanted into the detection chamber. The practical feasibility of the proposed CD device for clinical applications has been demonstrated by performing a creatinine test. It has been shown that the accurate determination of creatinine

concentration in the blood samples can be accomplished. Overall, the disk proposed in this study enables a precise quantitative plasma assay to be performed irrespective of the amount of plasma collected in the blood separation process. Moreover, the proposed microchannel structure can be easily integrated with other lab-on-a CD devices to realize a fully-functional lab-on-a-CD system for blood clinical diagnostic applications.

Acknowledgments The authors gratefully acknowledge the financial support provided to this study by the National Science Council of Taiwan under Grant No. NSC 101-2221-E-150-036. In addition, the access provided to the fabrication equipment used in the present study by the Common Lab for Micro/Nano Science and Technology of National Formosa University is also greatly appreciated.

References

- Andersson P, Jesson G, Kylberg G, Ekstrand G, Thorsén G (2007) Parallel nanoliter microfluidic analysis system. *Anal Chem* 79(11):4022–4030
- Arora A, Simone G, Salieb-Beugelaar GB, Kim JT, Manz A (2010) Latest developments in micro total analysis systems. *Anal Chem* 82(12):4830–4847
- Badr IHA, Johnson RD, Madou MJ, Bachas LG (2002) Fluorescent ion-selective optode membranes incorporated onto a centrifugal microfluidics platform. *Anal Chem* 74(21):5569–5575
- Blatter C, Jurischka R, Schoth A, Kerth P, Menz W (2005) Fabrication and testing of novel blood separation devices based on microchannel bend structures. *Proc SPIE* 5651:196–203
- Chen X, Cui DF, Liu CC, Li H (2007) Microfluidic chip for blood cell separation and collection based on crossflow filtration. *Sens Actuator B Chem* 130:216–221
- Chen CC, Lin PH, Chung CK (2014) Microfluidic chip for plasma separation from undiluted human whole blood samples using low voltage contactless dielectrophoresis and capillary force. *Lab Chip* 14:1996–2001
- Cho YK, Lee JG, Park JM, Lee BS, Lee YS, Ko C (2007) One-step pathogen specific DNA extraction from whole blood on a centrifugal microfluidic device. *Lab Chip* 7:565–573
- Chung KH, Choi YH, Yang JH, Park CW, Kim WJ, Ah CS, Sung GY (2012) Magnetically-actuated blood filter unit attachable to pre-made biochips. *Lab Chip* 12:3272–3276
- Dimov IK, Basabe-Desmonts L, Garcia-Cordero IL, Ross BM, Ricco AJ, Lee LP (2011) Stand-alone self-powered integrated microfluidic blood analysis system (SIMBAS). *Lab Chip* 11:845–850
- Ducrée J, Haeberle S, Brenner T, Glatzel T, Zengerle R (2005) Patterning of flow and mixing in rotating radial microchannels. *Microfluid Nanofluid* 2:97–105
- Focke M, Kosse D, Müller C, Reinecke H, Zengerle R, Von Stetten F (2010) Microstructuring of polymer films for sensitive genotyping by real-time PCR on a centrifugal microfluidic platform. *Lab Chip* 10:2519–2526
- Fung YC (1973) Stochastic flow in capillary blood vessels. *Microvasc Res* 5(1):34–38
- Gao L, Li J, Kasserra C, Song Q, Arjomand A, Hesk D, Chowdhury SK (2011) Precision and accuracy in the quantitative analysis of biological samples by accelerator mass spectrometry: application in microdose absolute bioavailability studies. *Anal Chem* 83(14):5607–5616
- Gorkin R, Park J, Siegrist J, Amasia M, Lee BS, Park JM, Kim J, Kim H, Madou M, Cho YK (2010) Centrifugal microfluidics for biomedical applications. *Lab Chip* 10(14):1758–1773

- Grumann M, Geipel A, Riegger L, Zengerle R, Ducrée J (2005) Batch-mode mixing on centrifugal microfluidic platforms. *Lab Chip* 5(5):560–565
- Haeberle S, Brenner T, Zengerle R, Ducrée J (2006) Centrifugal extraction of plasma from whole blood on a rotating disk. *Lab Chip* 6:776–781
- Hajmohammadi MR, Nourazar SS (2014) On the insertion of a thin gas layer in micro cylindrical Couette flows involving power-law liquids. *Int J Heat Mass Transf* 75:97–108
- Hajmohammadi MR, Eskandari H, Saffar-Avval M, Campo A (2013a) A new configuration of bend tubes for compound optimization of heat and fluid flow. *Energy* 62:418–424
- Hajmohammadi MR, Poozesh S, Nourazar SS, Manesh AH (2013b) Optimal architecture of heat generating pieces in a fin. *J Mech Sci Technol* 27:1143–1149
- Hajmohammadi MR, Nourazar SS, Campo A (2014a) Analytical solution for two-phase flow between two rotating cylinders filled with power law liquid and a micro layer of gas. *J Mech Sci Technol* 28:1849–1854
- Hajmohammadi MR, Rahmani M, Campo A, Joneydi Shariatzadeh O (2014b) Optimal design of unequal heat flux elements for optimized heat transfer inside a rectangular duct. *Energy* 68:609–616
- He H, Yuan Y, Wang W, Chiou NR, Epstein AJ, Lee LJ (2009) Design and testing of a microfluidic biochip for cytokine enzyme-linked immunosorbent assay. *Biomicrofluidics* 3:022401
- Huang Y, Joo S, Duhon M, Heller M, Wallace B, Xu X (2002) Dielectrophoretic cell separation and gene expression profiling on microelectronic chip arrays. *Anal Chem* 74:3362–3371
- Huang CT, Li PN, Pai CY, Leu TS, Jen CP (2010) Design and simulation of a microfluidic blood-plasma separation chip using micro-channel structures. *Sep Sci Technol* 45:42–49
- Inglis DW, Riehn R, Austin RH, Sturm JC (2004) Continuous microfluidic immunomagnetic cell separation. *Appl Phys Lett* 85:5093–5095
- Kersaudy-Kerhoasa M, Sollier E (2013) Micro-scale blood plasma separation: from acoustophoresis to egg-beaters. *Lab Chip* 13:3323–3346
- Kuo JN, Li BS (2014) Lab-on-CD microfluidic platform for rapid separation and mixing of plasma from whole blood. *Biomed Microdevices* 16:549–558
- Kuo JN, Lee WW, Chen JY (2012) Splitter microchannel network for equal plasma flow division on compact disk microfluidic chip. *Jpn J Appl Phys* 51:027201
- La M, Park SJ, Kim HW, Park JJ, Ahn KT, Ryew SM, Kim DS (2013) A centrifugal force-based serpentine micromixer (CSM) on a plastic lab-on-a-disk for biochemical assays. *Microfluid Nanofluid* 15:87–98
- Lai S, Wang S, Luo J, Lee LJ, Yang ST, Madou MJ (2004) Design of a compact disk-like microfluidic platform for enzyme-linked immunosorbent assay. *Anal Chem* 76:1832–1837
- Lee BS, Lee JN, Park JM, Lee JG, Kim S, Cho YK, Ko C (2009) A fully automated immunoassay from whole blood on a disc. *Lab Chip* 9:1548–1555
- Lee MG, Shin JH, Bae CY, Choi S, Park JK (2013) Label-free cancer cell separation from human whole blood using inertial microfluidics at low shear stress. *Anal Chem* 85:6213–6218
- Li C, Dong X, Qin J, Lin B (2009) Rapid nanoliter DNA hybridization based on reciprocating flow on a compact disk microfluidic device. *Anal Chim Acta* 640:93–99
- Lutz S, Weber P, Focke M, Faltin B, Hoffmann J, Müller C, Mark D, Roth G, Munday P, Armes N, Piepenburg O, Zengerle R, Von Stetten F (2010) Microfluidic lab-on-a-foil for nucleic acid analysis based on isothermal recombinase polymerase amplification (RPA). *Lab Chip* 10:887–893
- Madou M, Zoval J, Jia G, Kido H, Kim J, Kim N (2006) Lab on a CD. *Ann Rev Biomed Eng* 8:601–628
- Moorthy J, Beebe DJ (2003) In situ fabricated porous filters for microsystems. *Lab Chip* 3:62–66
- Petersson F, Nilsson A, Holm C, Jönsson H, Laurell T (2005) Carrier medium exchange through ultrasonic particle switching in microfluidic channels. *Anal Chem* 77(5):1216–1221
- Smistrup K, Hansen O, Bruus H, Hansen MF (2005) Magnetic separation in microfluidic systems using microfabricated electromagnets—experiments and simulations. *J Magn Magn Mater* 293:597–604
- Steigert J, Grumann M, Dube M, Streule W, Riegger L, Brenner T, Koltay P, Mittmann K, Zengerle R, Ducrée J (2006) Direct hemoglobin measurement on a centrifugal microfluidic platform for point-of-care diagnostics. *Sens Actuators A* 130–131:228–233
- Steigert J, Brenner T, Grumann M, Riegger L, Lutz S, Zengerle R, Ducrée J (2007) Integrated siphon-based metering and sedimentation of whole blood on a hydrophilic lab-on-a-disk. *Biomed Microdevices* 9:675–679
- Sun J, Liu C, Li M, Wang J, Xianyu Y, Hu G, Jiang X (2013) Size-based hydrodynamic rare tumor cell separation in curved microfluidic channels. *Biomicrofluidics* 7:011802
- Toner M, Irimia D (2005) Blood-on-a-chip. *Annu Rev Biomed Eng* 7:77–103
- Tsutsui H, Ho CM (2009) Cell separation by non-inertial force fields in microfluidic systems. *Mech Res Commun* 36(1):92–103
- Tüdös AJ, Besselink GAJ, Schasfoort RBM (2001) Trends in miniaturized total analysis systems for point-of-care testing in clinical chemistry. *Lab Chip* 1:83–95
- Van Delinder V, Groisman A (2006) Separation of plasma from whole human blood in a continuous cross-flow in a molded microfluidic device. *Anal Chem* 78:3765–3771
- Vilkner T, Janasek D, Manz A (2004) Micro total analysis systems. Recent developments. *Anal Chem* 76:3373–3386
- Yager P, Edwards T, Fu E, Helton K, Nelson K, Tam MR, Weigl BH (2006) Review article microfluidic diagnostic technologies for global public health. *Nature* 442:412–418
- Zhang J, Guo Q, Liu M, Yang J (2008) A lab-on-CD prototype for high-speed blood separation. *J Micromech Microeng* 18:125025
- Zhang XB, Wu ZQ, Wang K, Zhu J, Xu JJ, Xia XH, Chen HY (2012) Gravitational sedimentation induced blood delamination for continuous plasma separation on a microfluidics chip. *Anal Chem* 84(8):3780–3786